Communication

Helical Structure of Single-Crystalline ZnGaO Nanowires

Seung Yong Bae, Jinyoung Lee, Hyunsung Jung, Jeunghee Park, and Jae-Pyoung Ahn

J. Am. Chem. Soc., **2005**, 127 (31), 10802-10803• DOI: 10.1021/ja0534102 • Publication Date (Web): 13 July 2005

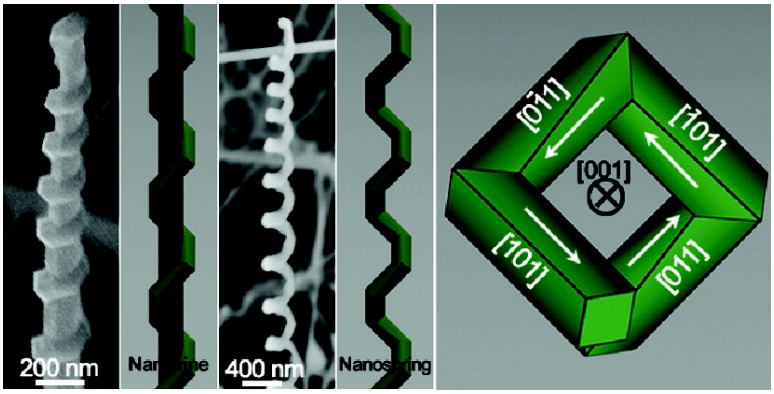

More About This Article

Additional resources and features associated with this article are available within the HTML version:

- Supporting Information
- Links to the 15 articles that cite this article, as of the time of this article download
- Access to high resolution figures
- Links to articles and content related to this article
- Copyright permission to reproduce figures and/or text from this article

View the Full Text HTML

J|A|C|S
COMMUNICATIONS

Published on Web 07/13/2005

Helical Structure of Single-Crystalline $ZnGa_2O_4$ Nanowires

Seung Yong Bae,[†] Jinyoung Lee,[†] Hyunsung Jung,[†] Jeunghee Park,*[,†] and Jae-Pyoung Ahn[‡]

Department of Chemistry, Korea University, Jochiwon 339-700, Korea, and Nano-Material Research Center, Korea Institute of Science and Technology, Seoul 136-791, Korea

Received May 25, 2005; E-mail: parkjh@korea.ac.kr

Since the discovery of carbon nanotubes (CNTs),[1] one-dimensional (1D) nanostructures have attracted a considerable amount of attention, due to their potential utilization as building blocks for electronic and photonic nanodevices.[2,3] Widening the use of these 1D nanostructures requires a greater assortment of structures to be made available. Recently, interest in curved quasi-1D nanostructures, such as helix/spring, ring, bow, and so forth, has been steadily increasing, owing to their attractive morphology and properties.[4−10] The helical CNTs can be used as extremely sensitive mechanical resonators to detect mass changes.[6] Despite the high expectations concerning their imminent application, however, the synthesis of other helical nanostructures has remained limited to ZnO, Si, and SiC materials.[7−10] Herein, we synthesize two novel helical zinc gallate ($ZnGa_2O_4$) nanostructures; helical $ZnGa_2O_4$ nanowire rolls either on a straight ZnSe nanowire support, which makes them look like "vines", or without any support, in which case they have the appearance of "springs". Thus, we refer to them as "nanovines" and "nanosprings", respectively. $ZnGa_2O_4$, which has a band gap (E_g) of 4.4−5.0 eV, is useful as a transparent conducting oxide in near-UV region.[11] Our research group previously reported the first synthesis of blue-light-emitting $ZnGa_2O_4$ nanowires.[12] In the present study, we focus on the structure analysis of the helical $ZnGa_2O_4$ nanowires based on their electron microscopy images.

Helical $ZnGa_2O_4$ nanostructures were synthesized by a two-step thermal evaporation method. (1) High-purity single-crystalline ZnSe nanowires were synthesized using CoSe (99%, Aldrich)/ZnO (99.98%, Aldrich) on a Au nanoparticles-deposited Si substrate at 800 °C (Supporting Information, Figure S1). (2) The pre-grown ZnSe nanowires were placed near the ZnO/Ga (99.99%, Aldrich), and a temperature of 600 or 900 °C was maintained for 10−60 min, thereby producing the $ZnGa_2O_4$ nanowires. The products were analyzed by scanning electron microscopy (SEM, Hitachi S-4700), transmission electron microscopy (TEM, FEI TECNAI G^2, 200 kV), high-voltage TEM (HVEM, JEOL JEM ARM 1300S, 1.25 MV), and energy-dispersive X-ray fluorescence spectroscopy (EDX).

Figure 1a shows an SEM image of the nanostructures grown at 600 °C. The magnified image reveals the nanovine structure in which the helical nanowire winds around the straight nanowire support (Figure 1b). Scanning TEM (STEM) and EDX line-scanning reveal that the nanovine is composed of helical $ZnGa_2O_4$ and straight ZnSe nanowires (Supporting Information, Figure S2). Figure 1c shows an SEM image of the springlike $ZnGa_2O_4$ nanostructures synthesized at 900 °C. The magnified image shows clearly the self-coiled morphology without any support (Figure 1d). Others are mostly unreacted ZnSe nanowires.

The TEM image explicitly shows a constant angle of the $ZnGa_2O_4$ nanowire over the entire helical structure (Figure 2a). The average diameter is 80 nm. Figure 2b corresponds to the magnified image, measured at the [100] zone axis, revealing that the [011] and [0$\bar{1}$1] growth directions of the helical $ZnGa_2O_4$ nanowire zigzag periodically, with an oblique angle (defined in the figure) of 45°.

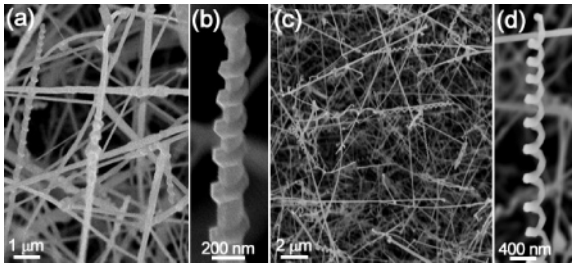

Figure 1. (a) SEM micrograph shows the wirelike morphology and (b) the magnified image shows that the helical nanowire is rolled around the straight nanowire. (c) High-density nanostructures are produced with (d) a self-coiled spring morphology.

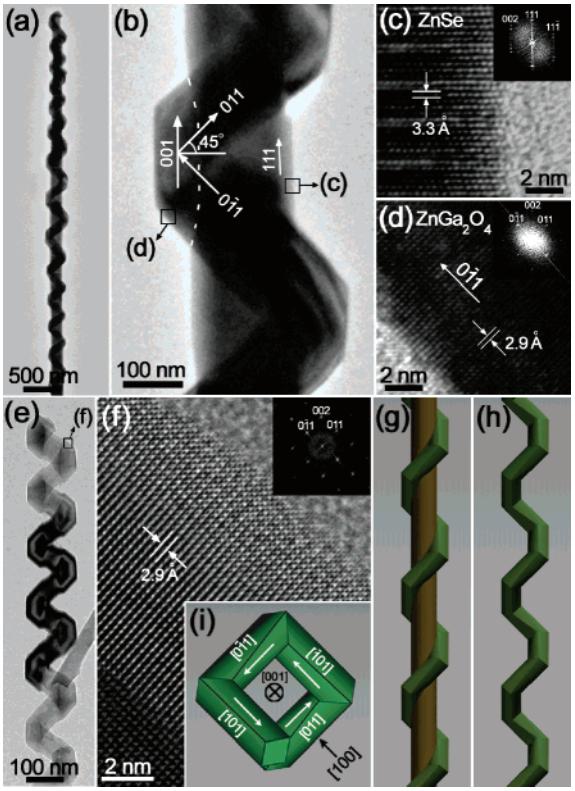

Figure 2. (a) TEM image shows the general morphology of the nanovines. (b) The growth direction of the helical nanowire changes zigzagged with a constant oblique angle of 45°. Atomic-resolved image and corresponding FFT ED pattern (inset) for (c) the straight ZnSe nanowire and (d) the helical $ZnGa_2O_4$ nanowire. (e) General morphology of the nanospring having a constant angle and pitch. (f) The single-crystalline $ZnGa_2O_4$ crystal has a [0$\bar{1}$1] growth direction, as confirmed by the FFT ED pattern (inset). Schematic models for (g) the nanovines and (h) the nanosprings. (i) Top-view diagram showing the four growth directions of the helical nanowires.

[†] Korea University.
[‡] Korea Institute of Science and Technology.

10.1021/ja0534102 CCC: $30.25

The [001] axial direction maintains along the whole length. The surface of the ZnSe nanowire is indented at its junction with the helical $ZnGa_2O_4$ nanowire, as indicated by the dotted line. Figure 2, parts c and d and their insets, shows the atomic-resolved images and fast-Fourier transformed electron diffraction (FFT ED) patterns for the parts marked in Figure 2b, proving that the nanovine is composed of a cubic ZnSe single crystal with a [111] ($d_{111} = 3.3$ Å) growth direction and a cubic $ZnGa_2O_4$ single crystal with a [$0\bar{1}1$] ($d_{022} = 2.9$ Å) growth direction. The corresponding lattice constant is consistent with that of the bulk crystal (ZnSe JCPDS No. 37-1463 and $ZnGa_2O_4$ JCPDS No. 38-1240). The HVEM image of the self-coiled $ZnGa_2O_4$ nanowire shows the zigzagged growth direction with the uniform angle and pitch (Figure 2e). Remarkably, the oblique angle (45°) and growth direction are the same as those of the nanovines. Its atomic-resolved image and FFT ED pattern confirm a defect-free single-crystalline $ZnGa_2O_4$ crystal with a [$0\bar{1}1$] growth direction (Figure 2f and its inset). It is noteworthy that both the nanovines and nanosprings are entirely composed of single-crystalline $ZnGa_2O_4$ crystals without any dislocation or distortion.

From the structure information provided, schematic models were constructed for the nanovines and nanosprings holding the identical $ZnGa_2O_4$ helical structure (Figure 2g,h). The helixes have highly symmetric and periodic structure, which results from the same length of building blocks. The top-view model shows that the blocks have four equivalent ⟨011⟩ directions: [011], [101], [$0\bar{1}1$], and [$\bar{1}01$], and there is a 90° rotation between two adjacent blocks (Figure 2i). These building blocks stack with an inclined angle of 45°, along the [001] axial direction. When the incident beam is parallel to the [100] direction, the TEM image shows only two zigzagged [011] and [$0\bar{1}1$] blocks. Further TEM analysis was performed carefully for another nanovine to confirm the uniform growth direction for all the helixes that we observed (Supporting Information, Figures S3 and S4).

The Wang group reported that single-crystalline wurtzite ZnO nanohelixes have six equivalent growth directions of ⟨$0\bar{1}11$⟩ due to their polarity.[7c] They explained that the sequential change in the growth direction is formed to reduce the electrostatic interaction energy caused by the ±{$01\bar{1}1$} polar surfaces of the nanowires. In contrast, the helical $ZnGa_2O_4$ nanowires described in the present study have four equivalent ⟨011⟩ growth directions. Considering their nanovine structures, we conjecture that lattice matching occurs when the $ZnGa_2O_4$ nanowire winds around the ZnSe nanowire. The interlayer distances of the (022) and (400) planes of $ZnGa_2O_4$ are 2.946 and 2.083 Å, respectively, corresponding to its growth direction and zone axis. The (002) and (220) planes of the ZnSe nanowires, which are lying along the growth direction and zone axis of the $ZnGa_2O_4$ nanowires, respectively, are separated by distances of 2.835 and 2.004 Å. The lattice mismatch between the (022) $ZnGa_2O_4$ and (002) ZnSe planes, and that between the (400) $ZnGa_2O_4$ and (220) ZnSe planes, are only about 4%. Therefore, it would be expected for the helical $ZnGa_2O_4$ crystal to grow in the ⟨011⟩ direction, due to the lattice matching with the ZnSe crystal.

The straight $ZnGa_2O_4$ nanowires were synthesized using ZnO/Ga at 900−1000 °C.[12] In comparison, the $ZnGa_2O_4$/ZnSe nanovines are produced at a lower temperature of 600 °C. The indented surface of the ZnSe nanowire, as shown in Figure 2b (or Supporting Information, Figure S3), indicates that the surface of the ZnSe nanowire may have melted to supply the Zn, thereby helping to grow the helical $ZnGa_2O_4$ nanowire at the lower temperature. This scenario is related to the growth model in which the Au nanoparticle acts as a catalyst to melt the Zn and moves along the surface of the ZnSe nanowire during the growth of the $ZnGa_2O_4$ nanowire (Supporting Information, Figure S5). Moreover, the lattice matching between the $ZnGa_2O_4$ and ZnSe crystals could play a critical role in determining the growth direction. The $ZnGa_2O_4$ nanosprings may be produced by the mechanism in which the ZnSe nanowires induce the growth of the $ZnGa_2O_4$ nanowires such as the nanovines and then ultimately evaporate afterward due to a high temperature of 900 °C.

The ZnSe ($E_g = 2.7$ eV at 300 K) nanowires exhibit a band-edge emission at 2.7 eV and a stronger emission at 2.0 eV associated with defects (Supporting Information, Figure S6).[13] The $ZnGa_2O_4$ nanowires have a blue emission at 3.1 eV, originating from the self-activation center of the octahedral Ga−O.[12] We anticipate that the $ZnGa_2O_4$/ZnSe nanovines could be used as a distinctive multicolored light-emitting-diode nanomaterial. The $ZnGa_2O_4$ nanosprings could be used as more efficient sensing materials or mechanical resonators.

In summary, we synthesized $ZnGa_2O_4$/ZnSe nanovines and $ZnGa_2O_4$ nanosprings by thermal evaporation using the ZnSe nanowires. Both the nanovines and nanosprings have a common structure, in which the growth direction of the helical $ZnGa_2O_4$ nanowire changes zigzagged with the same angle. They all consist of single-crystalline cubic $ZnGa_2O_4$ crystals without any dislocation over the entire helical structure and have four equivalent ⟨011⟩ growth directions: [011], [101], [$0\bar{1}1$], and [$\bar{1}01$], with the [001] axial direction. We suggest that the lattice matching with the ZnSe nanowires is an important factor in determining the growth direction of the helical $ZnGa_2O_4$ nanowires.

Acknowledgment. This work was supported by KOSEF (R14-2003-033-01003-0; R02-2004-000-10025-0) and KRF (2003-015-C00265). The SEM and HVEM analyses were performed at KBSI.

Supporting Information Available: SEM/TEM/XRD data of the ZnSe nanowires, STEM/EDX of the $ZnGa_2O_4$/ZnSe nanovines, schematic model of the helix, growth model of the $ZnGa_2O_4$/ZnSe nanovines, and PL spectrum. This material is available free of charge via the Internet at http://pubs.acs.org.

References

(1) Iijima, S. *Nature* **1991**, *354*, 56.
(2) Duan, X.; Huang, Y.; Cui, Y.; Wang, J.; Lieber, C. M. *Nature* **2001**, *409*, 66.
(3) Gudiksen, M. S.; Lauhon, L. J.; Wang, J.; Smith, D. C.; Lieber, C. M. *Nature* **2002**, *415*, 617.
(4) (a) Amelinckx, S.; Zhang, X. B.; Bernaerts, D.; Zhang, X. F.; Ivanov, V.; Nagy, J. B. *Science* **1994**, *265*, 635. (b) Gao, R.; Wang, Z. L.; Fan, S. *J. Phys. Chem. B* **2000**, *104*, 1227. (c) Bajpai, V.; Dai, L,; Ohashi, T. *J. Am. Chem. Soc.* **2004**, *126*, 5070.
(5) Zhang, G.; Jiang, X.; Wang, E. *Appl. Phys. Lett.* **2004**, *84*, 2646.
(6) Volodin, A.; Buntinx, D.; Ahlskog, M.; Fonseca, A.; Nagy, J. B.; Van Haesendonck, C. *Nano Lett.* **2004**, *4*, 1775.
(7) (a) Kong, X. Y.; Wang, Z. L. *Nano Lett.* **2003**, *3*, 1625. (b) Kong, X. Y.; Ding, Y.; Yang, R. S.; Wang, Z. L. *Science* **2004**, *303*, 1348. (c) Yang, R.; Ding, Y.; Wang, Z. L. *Nano Lett.* **2004**, *4*, 1309. (d) Hughes, W. L.; Wang, Z. L. *J. Am. Chem. Soc.* **2004**, *126*, 6703.
(8) Tang, Y. H.; Zhang, Y. F.; Wang, N.; Lee, C. S.; Han, X. D.; Bello, I.; Lee, S. T. *J. Appl. Phys.* **2001**, *85*, 7981.
(9) Zhang, H.-F.; Wang, C.-M.; Wang, L.-S. *Nano Lett.* **2002**, *2*, 941.
(10) Zhang, D.; Alkhateeb, A.; Han, H.; Mahmood, H.; Mcllroy, D. N.; Norton, M. G. *Nano Lett.* **2003**, *3*, 983.
(11) (a) Hsieh, I. J.; Chu, K. T.; Yu, C. F.; Feng, M. S. *J. Appl. Phys.* **1994**, *76*, 3735. (b) Jeong, I.-K.; Park, H. L.; Mho, S.-I. *Solid State Commun.* **1998**, *105*, 179.
(12) Bae, S. Y.; Seo, H. W.; Na, C. W.; Park, J. *Chem. Commun.* **2004**, 1834.
(13) (a) Zhu, Y.-C.; Bando, Y. *Chem. Phys. Lett.* **2003**, *377*, 367. (b) Zhang, X. T.; Liu, Z.; Ip, K. M.; Leung, Y. P.; Li, Q.; Hark, S. K. *J. Appl. Phys.* **2004**, *95*, 5752.

JA0534102